

## Nanometer-scale electrochromic properties observed by scanning near-field optical microscopy capable of local current sensing

Futoshi Iwata, Katsunari Mikage, Hiroshi Sakaguchi\*,  
Michihiko Kitao\* and Akira Sasaki

Faculty of Engineering, Shizuoka University, Johoku Hamamatsu 432-8561, Japan  
Fax: 81-53-478-1072, e-mail: tmfiwat@ipc.shizuoka.ac.jp

\*Research Institute of Shizuoka University, Johoku Hamamatsu 432-8011, Japan

A novel scanning near-field optical microscopy (SNOM) capable of point-contact current sensing was developed to investigate the nanometer-scale electrochromic (EC) behaviors of EC thin film. In order to detect the current and the optical signal at a local point on the surface, a cantilever type metal probe was fabricated. The near-field optical property could be detected by using the local field enhancement effect generated at the edge of the metal probe under p-polarized laser illumination. The current signal could be detected with a high-sensitive current amplifier connected with the metal probe. As the performance of the novel microscope, EC thin films of  $\text{WO}_3$  were observed. Using the current sensing SNOM, the surface topography, conductive image and optical distribution of the colored EC thin film were observed. Nanometer-scale EC properties accompanied with local bleaching behaviors could be investigated using the current-sensing SNOM.

Key words: Electrochromic film, Scanning near-field microscopy, atomic force microscopy

### 1. INTRODUCTION

The reversible coloration/bleaching phenomenon resulting from an electrochemical redox reaction is known as electrochromism. Electrochromic (EC) materials are expected to find many applications such as switchable windows, display devices and solar energy. Since the phenomenon was first found out by Deb[1], the properties of  $\text{WO}_3$  films, the most typical EC materials, have been widely investigated. Many researchers have investigated with respect to EC coloration procedure by the measurements of ESR[2], IR absorption[3,4,5] and Raman spectroscopy[6,7]. On the other hand, observation of EC films in microscopic real space is very attractive because microscopic structures of EC films depend on the film preparation conditions, which might strongly influence the EC properties. Atomic force microscopy (AFM) is an excellent tool for observation of surface topography in nanometer scale spatial resolution. Recently, EC films have been observed using AFM. Relations of the nanometer-scale structures and EC properties have been reported[8]. However, in order to investigate the local optical properties of such photonic functionalized materials, it is important to observe not only topographical information but also local optical properties. Furthermore in the case of EC materials, local electric properties also should be observed because coloration and electrical properties are strongly related in the EC materials. Scanning near-field optical microscope (SNOM) can provide information on the characteristics of surface optical properties with a spatial resolution on subwavelength scale. However, it is impossible to obtain the surface electric properties at the local area.

In this paper, we describe the development of the current sensing SNOM system for evaluation of local electrical and optical properties of EC materials. The

current sensing SNOM can provide not only surface optical information but also surface electronic properties at the local area. The preliminary observations of topography, current image and optical image of the colored  $\text{WO}_3$  films are performed. Nanometer-scale optical and electrical behaviors of the  $\text{WO}_3$  thin films are discussed.

### 2. EXPERIMENTAL APPARATUS AND METHOD

#### 2.1 Current sensing SNOM

Figure 1 shows a schematic diagram of a current-sensing SNOM. The current-sensing SNOM used in the present experiment was a homemade apparatus for observation of the local electrical and optical properties of EC materials. The metal probe has to serve multiple functions: force sensing, optical signal, and conductivity. Thus, a conductive and bent-type metal probe was fabricated in order to realize a cantilever operation in AFM tapping mode. The fabrication process is as follows. The Pt-Rh wire, which for our purposes was of diameter 0.10 mm, first had to be bent, then the apex of the  $80^\circ$  bending probe was sharpened using two steps electrochemical etching process. As the first process, the edge of the bent wire was submerged 1.0 mm into the etching solution that consists of saturated  $\text{CaCl}_2$  (60% by volume,  $\text{H}_2\text{O}$  (35%), and  $\text{HCl}$  (5%). The submerged wire edge was etched against a carbon electrode at 20 V ac. The first etching was continued until only a few bubbles emerge from the probe. Then, as the second step, the edge of the probe was touched with the etchant thin film held in a gold wire loop. The loop 3 mm in diameter made from 0.1 mm gold wire, was raised and lowered with respect to the edge of the probe with applying ac potential of 1-2V, which acts as precision micropolishing. This etching process realizes the small radius of curvature (<50 nm).

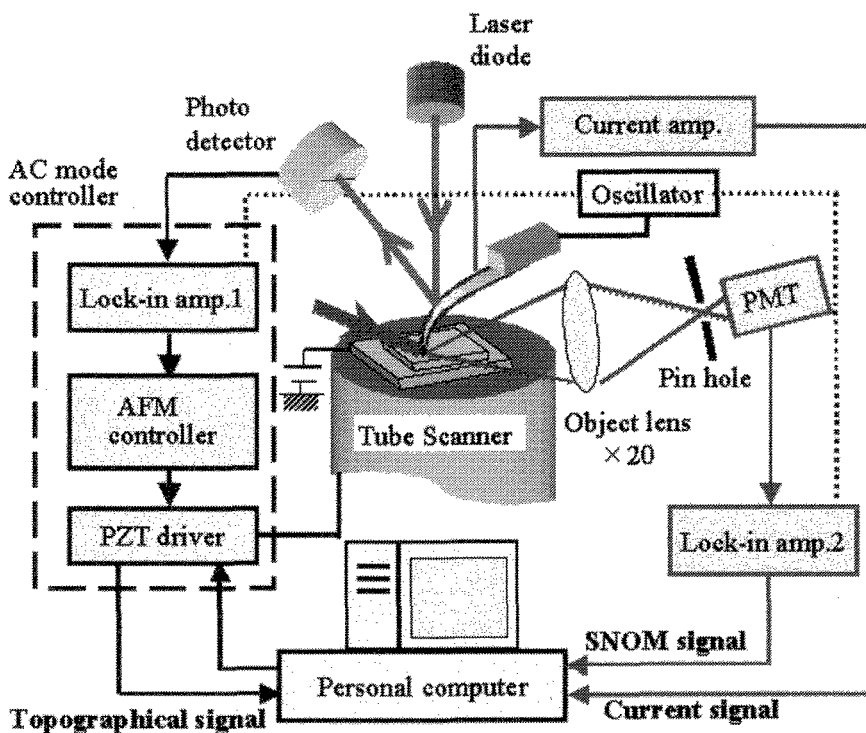


Fig. 1 Schematic diagram of the current sensing SNOM

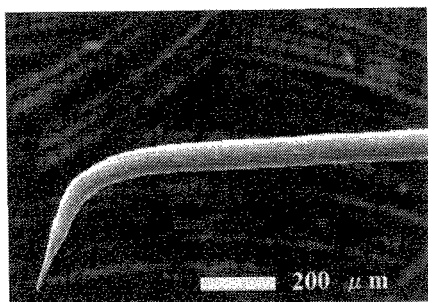


Fig. 2 SEM image of the fabricated Pt-Rh probe

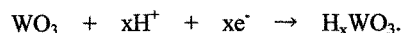
The fabricated Pt-Ir probe is shown in Fig. 2.

With respect to detection method of the near field optical signal, apertureless type SNOM was constructed with the combination of the metal probe and laser beam[9]. It has been theoretically shown that when a metal probe is illuminated by a laser light whose electric field is polarized mainly parallel to the probe axis, a large charge concentration occurs at the probe end, resulting in a strong localized Field Enhancement (FE)[10]. The intensity of the enhanced field can reach several thousands times the intensity of the incident light. The FE localization depends on the size and can be confirmed within an area of tens of nanometers of diameter. In this experiment, a collimated laser beam was irradiated to the sharpened edge of the Pt-Rh probe. The incident angle was 80 degrees with respect to the probe axis and electric field was mainly oriented along the probe axis. The localized optical signal at the vicinity of the probe edge was collected with the object

lens ( $\times 20$ , Mitutoyo Co., Ltd.), then, it was detected with the photo multiplier tube (PMT). In order to remove the back ground noise, the optical intensity was modulated using vertically oscillating probe in tapping mode. Then the modulated signal could be detected with a lock-in amplifier. The local electric current is detected by the Pt-Rh probe connected to a high-speed current-sensing amplifier with a response time  $10 \mu\text{s}$  and a detection limit of  $0.1 \text{ pA}$  (model 1211, Ithaca Co., Ltd.). Therefore surface topography, current distribution and optical image could be observed, simultaneously.

## 2.2 Sample preparation of EC cells

$\text{WO}_3$  films were prepared by rf-sputtering from a metallic W target (10 cm in diameter, 99.9% purity) in a atmosphere consisting of argon and oxygen. The sputtering was carried out using rf magnetron sputtering equipment (Anelva SPF-332H). The rf power and the total pressure were  $1.27 \text{ W/cm}^2$  and 8 Pa, respectively. The substrates were ITO (Indium-Tin-Oxide)-coated glass plates. Average thickness of  $\text{WO}_3$  films was 500 nm. The electrochemical reaction due to double injection or extraction of electrons and protons is expressed by the chemical formula,



It is known from this formula that the coloration and bleaching processes correspond to reduction and oxidation reactions, respectively. The reduction process results in the formation of a blue-colored tungsten bronze  $\text{H}_x\text{WO}_3$ , where  $x$  is the atomic ratio of

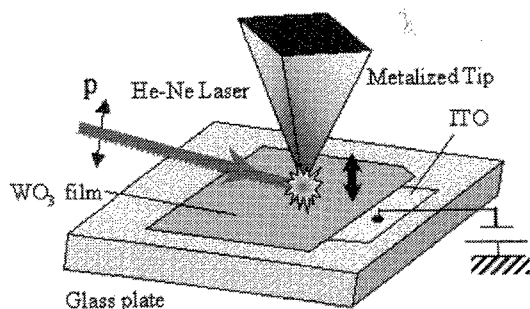


Fig. 3 Set up of the EC cell and metallic probe

hydrogen to tungsten.

Electrochemical coloration/bleaching (C/B) was performed in an electrolyte of 1N  $\text{H}_2\text{SO}_4$  ethanol solution. A carbon rod was used as a counter electrode. A voltage of  $\pm 1.5\text{V}$  was applied between the ITO and the counter electrode.

As for observation of the  $\text{WO}_3$  films, the colored  $\text{WO}_3$  films of the EC cells were set on the sample holder of the current sensing SNOM. As a illumination light, the collimated He-Ne laser, 633 nm wavelength and 3 mW output power, was irradiated to the probe because colored  $\text{WO}_3$  films show strong optical absorption at this wavelength. DC voltage was applied on the ITO electrode with respect to the probe. Local optical and electrical properties of the films were observed by scanning the probe of the current sensing SNOM as shown in Fig. 3.

### 3. RESULTS AND DISCUSSION

#### 3.1 Observation of the colored $\text{WO}_3$ film

Figures 4 show the topography, optical image and current image of the colored  $\text{WO}_3$  film, respectively. Those three images were observed, simultaneously. Figure 4(a) shows the surface topography of the  $\text{WO}_3$  film. The surface of the  $\text{WO}_3$  film consists of grains, which were formed by the sputtering process. The grains size are about 100-300 nm in diameters. Figure 4(b) shows the near-field optical image at the same area of the topographical image of Fig. 4(a). As shown in this figure, even smaller grain size compared with the wavelength of the He-Ne laser (670 nm), the individual grains can be seen clearly due to high spatial resolution of near-field optics. In this image, the dark part indicates lower reflective area, which means higher optical absorption area. Thus this optical image indicates almost all grains absorb the light of the He-Ne laser due to colored state of the  $\text{WO}_3$  film. Figure 4(c) shows current image at the same area of Fig. 4(a) and (b). The dark area indicates the part at where large current was detected. Thus dark area means highly charge injected area at the electrochemically colored process of the sample preparation. In this image, almost all the grains are electrically charged. Those charged grains in Fig. 4(c) agree well with the colored grains in the optical image in Fig. 4(b). Therefore, by using the current sensing SNOM, it is possible to observe that the individual grains of the  $\text{WO}_3$  film are electrically charged and colored at the coloration state.

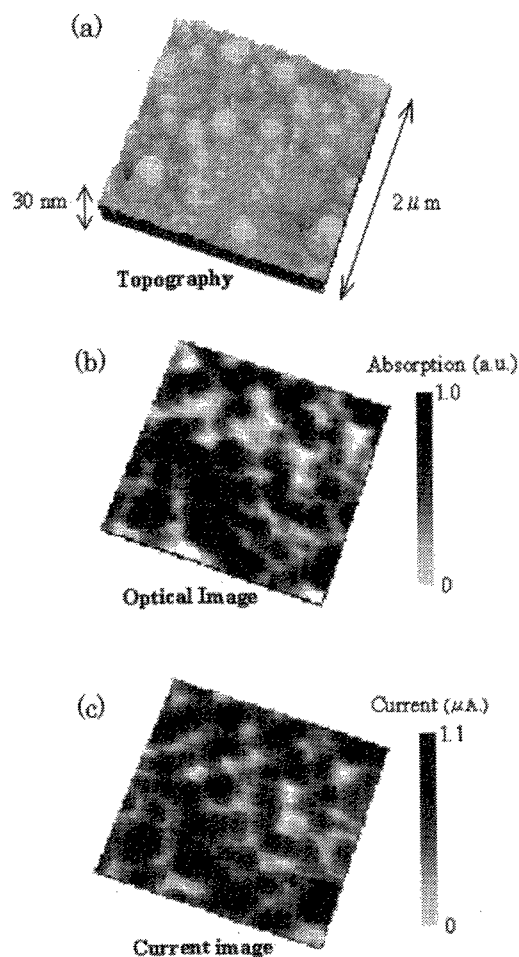


Fig. 4 (a)Topography, (b) optical image and (c)current image of the colored  $\text{WO}_3$  film.

#### 3.2 Local bleaching modification

In order to observe nanometer-scale EC phenomenon, we tried to bleach at the local area of the colored  $\text{WO}_3$  film using the current sensing SNOM. On the surface of the charged  $\text{WO}_3$  film at the colored state, the injected charge was locally extracted by the probe with applying voltage of 2 V. The Pt-Rh probe was scanned at the small area for local bleaching. Then the modified surface was observed with the SNOM. Figure 5(a) and (b) show the topography and optical image of the locally bleached surface of the  $\text{WO}_3$  film, respectively. The square in the image indicates the previously scanned area for the local extraction (bleaching) process. In the topographical image, the morphology of the pre-scanned area is almost the same as that of the outside square. However, as shown in Fig. 5(b), the contrast of the inside square indicates brighter than that of the outside square in the optical image, which means lower optical absorption at the area. Therefore local bleaching could be successfully performed on the surface by the novel technique of the current sensing SNOM. In the optical image, the bleaching phenomenon is seen at the individual grain level. Thus local bleaching might occurs at the individual grain level.

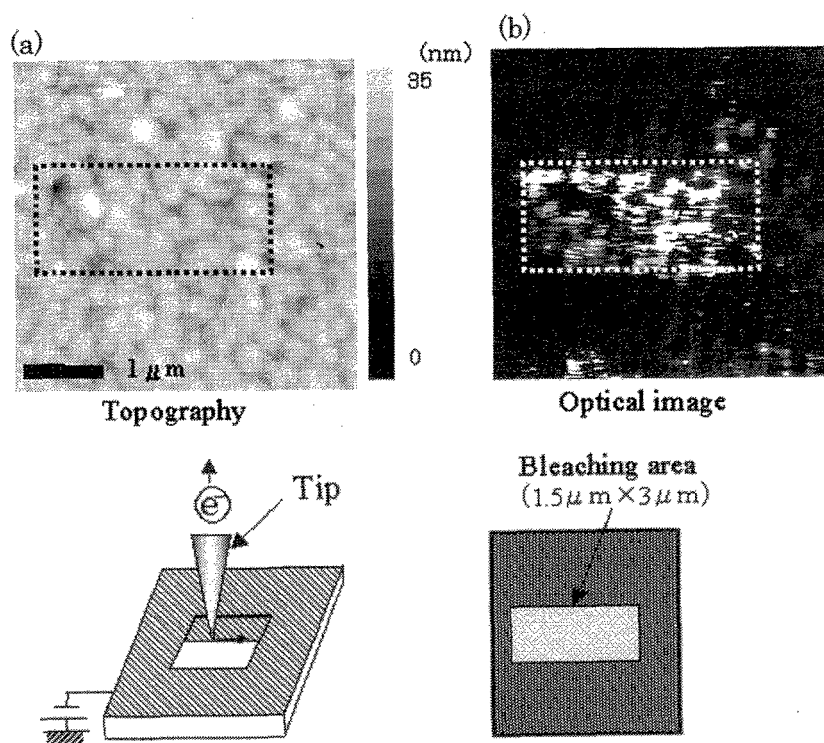


Fig. 5 Local bleached surface of the  $\text{WO}_3$  film

With respect to conventional bleaching process of  $\text{WO}_3$  films of EC cells, general bleaching is carried out in electrolyte solutions as electrochemical reaction. To keep the electronic neutrality, the same amount of electrons and ions are extracted from  $\text{WO}_3$  films. On the other hand, in this experiment of the local bleaching process using the current sensing SNOM, bleaching was carried out in the air atmosphere at the room temperature. In such environment, nanometer-scale surfaces are covered with very thin water film. Utilizing the water thin film, nanometer-scale surface modifications based on local electrochemical reactions have been performed using scanning tunneling microscope and AFM[11,12]. Therefore, in this case of the local bleaching of the  $\text{WO}_3$  film, small amount of protons might be diffused into the water thin film due to the local electrochemical reaction. Therefore, the nanometer-scale EC properties could be observed using the current sensing SNOM. It is very interesting to elucidate local EC properties and its applications in micro and nanometer-scale fields. More detail experiments of the local EC phenomena can be expected in future investigations.

#### 4. CONCLUSION

Local electrical and optical properties of  $\text{WO}_3$  films of the EC cell were observed with the current sensing SNOM. The current sensing SNOM, developed for local evaluation of EC materials, can provide not only optical information but also electrical properties in nanometer-scale spatial resolution. As for observation of the  $\text{WO}_3$  films at the colored state, the colored and charged grains could be observed clearly. Furthermore, local bleaching of the  $\text{WO}_3$  films were successfully performed with the current sensing SNOM. The bleaching phenomenon could be seen at the individual grains in the near-field optical image.

#### Acknowledgements

The authors wish sincerely to thank Mr. K. Urabe for his technical help of sputtering. This work was supported in part by Grants-in-Aid from the ministry of education, science and culture of Japan and Saneyoshi scholarship foundation.

#### References

- [1] S. K. Deb, *Philos. Mag.*, **27**, 801 (1973).
- [2] P. Gerard, A. Deneuille, R. Courthès, *Thin Solid Films* **71**, 221 (1980).
- [3] M.A. Habib, S. P. Maheswari, *J. Electrochem. Soc.*, **138** 2029 (1991).
- [4] M. Kitao, S. Yamada, S. Yoshida, H. Akram, K. Urabe, *Solar Energy Mater. Solar Cells* **25**, 241 (1992).
- [5] J. L. Paul, J. C. Lassegues, *J. Solid State Chem.* **106**, 357 (1993).
- [6] M. F. Daniel, B. Desbat, J. C. Lassegues, R. Garie, *J. Solid State Chem.* **73**, 127 (1988).
- [7] M. Ohtsuka, N. Goto, N. Sato, *J. Electronal. Chem.* **287**, 249 (1990).
- [8] M. Kitao, M. Makifuchi and A. Urabe, *Solar Energy Mater. Solar Cells* **70**, 219-30 (2001).
- [9] Y. Inouye and S. Kawata, *Opt. Lett.*, **19**, 159 (1994).
- [10] H. Furukawa and S. Kawata, *Opt. Commun.*, **15**, 221 (1998).
- [11] K. Matsumoto, S. Takahashi, M. Ishii, M. Hoshi, A. Kurokawa, S. Ichimura and A. Ando, *Jpn. J. Appl. Phys.* **34**, 1387 (1995).
- [12] J. A. Dagata, T. Inoue, J. Itoh, K. Matsumoto and H. Yokoyama, *J. Appl. Phys.* **84**, 6891 (1998).